


RESEARCH

Open Access



Cardiac involvement in COVID-19 patients: mid-term follow up by cardiovascular magnetic resonance

Hui Wang^{1†}, Ruili Li^{2†}, Zhen Zhou¹, Hong Jiang¹, Zixu Yan¹, Xinyan Tao¹, Hongjun Li^{2*} and Lei Xu^{1*} 

Abstract

Background: Coronavirus disease 2019 (COVID-19) induces myocardial injury, either direct myocarditis or indirect injury due to systemic inflammatory response. Myocardial involvement has been proved to be one of the primary manifestations of COVID-19 infection, according to laboratory test, autopsy, and cardiovascular magnetic resonance (CMR). However, the middle-term outcome of cardiac involvement after the patients were discharged from the hospital is yet unknown. The present study aimed to evaluate mid-term cardiac sequelae in recovered COVID-19 patients by CMR

Methods: A total of 47 recovered COVID-19 patients were prospectively recruited and underwent CMR examination. The CMR protocol consisted of black blood fat-suppressed T2 weighted imaging, T2 star mapping, left ventricle (LV) cine imaging, pre- and post-contrast T1 mapping, and late gadolinium enhancement (LGE). LGE were assessed in mixed both recovered COVID-19 patients and healthy controls. The LV and right ventricle (RV) function and LV mass were assessed and compared with healthy controls.

Results: A total of 44 recovered COVID-19 patients and 31 healthy controls were studied. LGE was found in 13 (30%) of COVID-19 patients. All LGE lesions were located in the mid myocardium and/or sub-epicardium with a scattered distribution. Further analysis showed that LGE-positive patients had significantly decreased LV peak global circumferential strain (GCS), RV peak GCS, RV peak global longitudinal strain (GLS) as compared to non-LGE patients ($p < 0.05$), while no difference was found between the non-LGE patients and healthy controls.

Conclusion: Myocardium injury existed in 30% of COVID-19 patients. These patients have depressed LV GCS and peak RV strains at the 3-month follow-up. CMR can monitor the COVID-19-induced myocarditis progression, and CMR strain analysis is a sensitive tool to evaluate the recovery of LV and RV dysfunction.

Keywords: COVID-19, Cardiac involvement, Cardiac dysfunction, Cardiac magnetic resonance imaging

Introduction

Coronavirus disease 2019 (COVID-19) is a nascent pandemic. Until July 20, 2020, 14,353,494 confirmed cases, including 603,703 deaths, were reported to the World Health Organization [1]. Data from previous studies suggested that acute cardiac injury occurred in 20% COVID-19 patients [2]. In hospitalized patients, the cardiac injury was up to 30% and caused 40% deaths [3–6]. The mechanisms of cardiac injury are direct myocarditis (direct myocardial infection by SARS-CoV-2) or indirect factors,

*Correspondence: leixu2001@hotmail.com; lihongjun00113@126.com

†Hui Wang and Ruili Li contributed equally to this work

¹ Department of Radiology, Beijing Anzhen Hospital, Capital Medical University, No. 2, Anzhen Road, Chaoyang, Beijing 100029, China

² Department of Radiology, Beijing Youan Hospital, Capital Medical University, No. 8, Xi Tou Tiao Youanmen Wai, Fengtai, Beijing 100069, China



such as cardiac stress due to respiratory failure, indirect injury from systemic inflammatory response-cytokine release syndrome, stress cardiomyopathy, or a combination of all these factors [6–9].

Cardiovascular magnetic resonance (CMR) can visualize and quantify heart volume and function and characterize the myocardial tissue; thus, it has been used as a gold standard non-invasive imaging tool in cardiovascular medicine [10]. A recent single-center study from Wuhan demonstrated that more than half of the recovered COVID-19 patients sustain cardiac edema, fibrosis, and impaired right ventricle (RV) contractile function [11]. However, in this small-sample retrospective study, only patients with reported cardiac symptoms were included. The middle-term outcome of cardiac involvement in COVID-19 patients is yet unknown. Thus, the present study aimed to evaluate mid-term cardiac sequelae in recovered COVID-19 patients by CMR.

Methods

Study design and participants

For this prospective, single-center study, we recruited consecutive COVID-19 patients from May 8 to July 20, 2020. The inclusion criteria were as follows: (1) confirmed to have SARS-CoV-2 infection, (2) recovered from COVID-19 and discharged from the hospital for 12 weeks, (3) agreed to participate and signed informed consent. The exclusion criteria were as follows: (1) pacemaker placement, (2) uncontrolled hypertension, (3) coronary artery disease (evidence of coronary artery stenosis > 50%) or previous myocardial infarction, (4) moderate to severe valvular dysfunction, (5) previous atrial fibrillation, (6) previous heart failure, (7) previous myocarditis, (8) known cardiomyopathy, (9) severe renal insufficiency (creatinine clearance rate < 30 mL/min/1.73 m²), (10) unable to cooperate with breath-holding and cannot undergo CMR examination, (11) pregnancy, (12) not suitable due to other factors.

Age- and sex-matched healthy controls, who previously underwent CMR in our hospital were selected from a health screening database. All the controls had a normal electrocardiogram (ECG), echocardiography, and CMR and did not present any cardiovascular disease or systemic inflammation. The present study was approved by the local institutional review board (KS2020001), and informed consent was obtained from all patients.

CMR scanning protocol

All patients underwent CMR on a 3 T CMR scanner (Ingenia CX, Philips Healthcare, Best, The Netherlands). The CMR protocol consisted of black blood fat-suppressed T2 weighted imaging (T2w), T2 star mapping, left ventricle (LV) cine imaging including four chambers,

two-chamber, short axis, pre- and post-contrast T1 mapping, and late gadolinium enhancement (LGE).

Black blood T2w imaging was performed in short axis using multishot turbo spin echo (TSE) sequence with time of repetition (TR)=2 heart beat periods, time of echo (TE)=75 ms, voxel size=1.7 × 1.7 × 8 mm³, field of view (FOV)=380 × 380 mm², flip angle (FA)=90°, and acceleration factor=2. T2 star mapping was carried out by a turbo field echo (TFE) sequence with 15 TEs from 1.15 to 16 ms, TR=29 ms, voxel size=1.8 × 1.8 × 15 mm³, FOV=300 × 300 mm², FA=25°, and acceleration factor=3. The cine scanning was conducted by a balanced steady state-free precession (bSSFP) sequence, with TR/TE=3.0/1.52 ms, FA=45°, voxel size=1.8 × 1.8 × 8 mm³, FOV=270 × 270 mm², and acceleration factor=1.5 or 3.6 depending on the number of slices acquired per breath hold. For short axis cine imaging, 9 slices were acquired to cover the entire LV. Modified Look-locker inversion recovery (MOLLI) acquisition scheme was applied for both pre- and post-contrast T1 mapping using single-shot bSSFP sequence with TR/TE=3.3/1.5 ms, voxel size=2 × 2 × 15 mm³, FOV=300 × 300 mm², FA=20°, and acceleration factor=2. LGE imaging was implemented 10 min after intravenous administration of contrast medium (0.2 mmol/kg; Magnevist gadopentetate dimeglumine, Bayer Healthcare, Bayer, Berlin, Germany) using a phase-sensitive inversion-recovery (PSIR) TFE sequence with TR/TE=6.1/3.0, voxel size=1.6 × 1.9 × 8 mm³, FOV=350 × 350 mm², FA=25°/5°, and acceleration factor=2. All the protocols were executed using ECG trigger and breath holding.

CMR images analysis

Both COVID-19 and healthy subject data were intermingled. And anonymized images were evaluated by 3 radiologists (ZZ, HW and LX with 5, 8 and 12 years of CMR diagnosis experience, respectively). The LGE lesion was quantified using full width at half-maximum method [12]. The visual presence and different patterns (epicardial, mid-wall, or transmural) on the LGE images were assessed by three radiologists independently. Any discrepancies were resolved by consensus. The ratio between the LGE volume and the total LV myocardium volume (LGE/myocardium) in the LGE-positive patients was calculated.

Whole LV myocardium region (including regions of LGE lesion) were delineated on the native T1 mapping and global T1 values were computed using cvi42 software (Circle Cardiovascular Imaging Inc., Calgary, Alberta, Canada).

The LV and RV function and LV mass were assessed based on the short-axis cine images using cvi42

software (Circle Cardiovascular Imaging). Endocardial and epicardial borders, with papillary muscles excluded from volumes, were identified automatically by the software and amended by a radiologist (HW). LV and RV range were defined from the planes of the mitral valve and tricuspid valve to the apex, respectively, on 4-chamber cine images in both diastolic and systolic phases. Short-axis images were divided into size-based equiangular segments with RV-LV junction as the reference point. LV and RV function parameters, end-diastolic volume (EDV), end-systolic volume (ESV), stroke volume (SV), cardiac output (CO), ejection fraction (EF), and LV mass were calculated automatically. All volumes and masses were normalized to the body surface area (BSA).

Three-dimensional (3D) global radial strain (GRS), global circumferential strain (GCS), and global longitudinal strain (GLS) of LV and RV were obtained using cvi42 (Circle Cardiovascular Imaging). The end-diastolic phase served as the reference. Contours of endo- and epicardial myocardium of short-axis, as well as the 2-, 3-, 4-chamber long-axis cine images, were drawn by two radiologists (HW and ZZ respectively). Patients were further divided into two subgroups based on the presence of LGE.

Statistical analysis

All data were analyzed using SPSS (version 25.0, Statistical Package for the Social Sciences, International Business Machines, Inc., Armonk, New York, USA). Normally distributed continuous variables were expressed as mean \pm standard deviation. Two-tailed one-way ANOVA was used to analyze the differences between LGE, non-LGE, and normal control groups. Categorical variables were expressed as counts and percentages. T-test was used to compare the means with normal distribution, and the Mann–Whitney U test was used to compare the variables with non-normal distribution between LGE and non-LGE groups. χ^2 test was used to explore the statistical significance of CMR parameters among LGE, non-LGE, and normal control groups. A two-sided $p < 0.05$ was considered as statistically significant.

Inter- and intra-observer intraclass coefficients (ICC) was used to assess reproducibility of strain measurements. The same investigator (HW) measured the 3D global strain of LV and RV in the all 75 studies on two occasions, separated by an interval of 2 months to assessment of intra-observer reproducibility. And a second investigator (ZZ) also evaluated all 75 subjects to assess inter-observer reproducibility.

Results

Population characteristics

From May 8 to July 20, 2020, 47 patients who recovered from COVID-19 were recruited and underwent CMR. One patient was excluded because of moderate tricuspid regurgitation, one was excluded because of hypertrophic cardiomyopathy, and one was excluded because of hypertensive cardiomyopathy. The resulting 44 recovered patients and 31 healthy controls were included in this study. The clinical characteristics of COVID-19 patients are reported in Table 1. The average age of COVID-19 patients was 47.6 ± 13.3 years, and the cohort comprised of 19 (43.2%) men. Among the 31 normal controls, 19 were male, which matched with the COVID-19 group. Although only 12 female healthy controls were included, there was no significant difference in sex distribution among patients with LGE-positive, patients with LGE-negative and normal controls ($P > 0.05$) (Table 2).

The average duration from discharge from the hospital to CMR examination was 102.5 ± 20.6 days. A quarter of the patients performed regular exercise, only one patient smoked, and three drank small amount alcohol every day (less than 25 mg per day). New York Heart Function Classification from I to IV was 21, 13, 8, 2, respectively. According to the Diagnosis and Treatment Protocol of Novel Coronavirus issued by the National Health Commission of the People's Republic of China [13], the moderate, severe, and critically ill types COVID-19 pneumonia were 32 of 44 (72.7%), 11 (25.0%), and 1 (2.3%), respectively; 11 (25.0%) patients had hypertension, 8 (18.2%) patients had diabetes, and 16 (36.4%) patients had hyperlipidemia before COVID-19. Non-patients had chronic obstructive pulmonary disease, cerebrovascular disease, or chronic renal diseases. Moreover, 2 (4.6%) patients had hepatitis B before COVID-19. Twenty-four (54.5%) patients were administered antiviral (Kaletra, Arbidol, oseltamivir, and interferon), 12 (27.3%) patients were given antibiotic (moxifloxacin, cefixime, and cefuroxime) and 13 patients were given corticosteroid therapy, while 10 (22.7%) patients were given high-flow oxygen support, 2 (4.6%) patients were administered intravenous immunoglobulin, and 2 (4.6%) were given angiotensin-converting enzyme inhibitors (ACEI) or angiotensin receptor blockers (ARB) (Table 1).

Among all 44 recovered patients, normal ECGs were revealed in 43 patients. ST segment elevation in leads II, III, AVF and prolonged PR interval during initial diagnosis was demonstrated in one patient. Echocardiography was performed in 5 patients, all showed a small amount of mitral or/and tricuspid regurgitation.

Table 1 Clinical characteristics, laboratory measurements, complications during hospitalization and treatment before discharge of recovered COVID-19 patients

Characteristic	Total COVID-19 patients (n = 44)	LGE (N = 13)	Non-LGE (N = 31)	P-value
Age (years)	47.6 ± 13.3	53.2 ± 14.5	45.2 ± 12.43	0.07
Gender	19 (43.2%)	4 (30.8%)	15 (48.4%)	0.34
BSA (kg/m ²)	1.76 ± 0.19	1.73 ± 0.17	1.77 ± 0.2	0.63
Heart rate (bpm)	66.2 ± 11.7	64.1 ± 6.8	67.0 ± 13.2	0.32
Time between hospital discharge and CMR (days)	102.5 ± 20.6	100.8 ± 20.3	103.3 ± 21.0	0.72
Regular exercise	10 (22.7%)	3 (23.1%)	7 (22.6%)	1.0
Smoke	1 (2.3%)	0	1 (3.2%)	NA
Alcohol	3 (6.8%)	1 (7.7%)	2 (6.5%)	1.0
NYHA I/II/III/IV	21/13/8/2	4/5/3/1	17/8/5/1	0.52
Clinical COVID-19 pneumonia types, moderate/severe/critical	32/11/1	7/5/1	25/6/0	0.10
Comorbidities				
Hypertension	11 (25.0%)	5 (38.5%)	6 (19.4%)	0.18
Diabetes mellites	8 (18.2%)	2 (15.4%)	6 (19.4%)	1.0
Hyperlipidemia	16 (36.4%)	3 (23.1%)	13 (41.9%)	0.31
Chronic obstructive pulmonary disease	0	0	0	NA
Cerebrovascular disease	0	0	0	NA
Chronic renal diseases	0	0	0	NA
Hepatitis B	2 (4.6%)	1 (7.7%)	1 (3.2%)	0.51
Laboratory findings				
CPK (u/l)*	69 (14–141)	57 (45–167)	76 (45–142)	0.85
CKMB (ng/ml)*	0.33 (0.18–0.64)	0.32 (0.11–0.73)	0.33 (0.19–0.64)	0.86
MYO (ng/ml)	56.8 ± 42.7	66.9 ± 59.7	52.6 ± 33.6	0.31
TnI (ng/ml)*	0.02 (0.01–0.02)	0.02 (0.01–0.04)	0.01 (0.01–0.02)	0.04
CRP (mg/l)	43 ± 43	55 ± 54	38 ± 37	0.24
Potassium (mmol/l)	3.8 ± 0.3	3.7 ± 0.3	3.8 ± 0.3	0.24
Calcium (mmol/l)	1.3 ± 0.2	1.3 ± 0.3	1.3 ± 0.2	0.33
Other complications during hospitalization				
cardiac arrhythmia	0	0	0	NA
Renal injury	4 (9.1%)	1 (7.7%)	3 (9.7%)	1.0
Liver injury	19 (43.2%)	5 (38.5%)	14 (45.2%)	0.68
Treatment before discharge				
Antiviral therapy	24 (54.5%)	9 (69.2%)	15 (48.4%)	0.21
Antibiotic therapy	12 (27.3%)	5 (38.5%)	7 (22.6%)	0.28
Corticosteroids	13 (29.6%)	6 (46.2%)	7 (22.6%)	0.12
Non-invasive ventilation of high-flow nasal cannula oxygen	10 (22.7%)	5 (38.5%)	5 (16.1%)	0.11
Intravenous immunoglobulin	2 (4.6%)	1 (7.7%)	1 (3.2%)	0.51
ACEI/ARB	2 (4.6%)	1 (7.7%)	1 (3.2%)	0.51

Boldface characters indicate $p < 0.05$

ACEI angiotensin converting enzyme inhibitor, ARB angiotensin receptor blocker, BSA body surface area, CMR cardiovascular magnetic resonance, CPK creatine phosphokinase, CRP C-reactive protein, LGE late gadolinium enhancement, MYO myohemoglobin, NYHA New York Heart Association, TnI troponin I

* Median (IQR)

Laboratory results

During hospitalization, troponin I (TnI), creatine phosphokinase (CPK), Creatine phosphokinase-MB (CPK-MB), myohemoglobin (MYO), C-reactive protein (CRP), serum potassium, and serum calcium were

measured in all patients at least one time. The median (interquartile range, IQR) or average ± standard deviation (SD) results of the highest value were as follows: TnI: 0.02 (0.01–0.02) ng/mL, CK: 69 (13.7–141.3) U/L, CKMB: 0.33 (0.18–0.64) ng/mL, MYO: 56.8 ± 42.7 ng/

Table 2 CMR parameters of recovered COVID-19 patients and normal controls

Characteristic	Total (n = 75)	COVID-19 patients (n = 44)		Healthy controls (n = 31)	P-Value*	Adjusted P-value**	Adjusted P-value***	Adjusted P-value****
		LGE-positvie (n = 13)	LGE-negative (n = 31)					
Age (years) Average ± SD	47.4 ± 12.3	53.2 ± 14.5	45.2 ± 12.3	47.1 ± 11.0	0.15	0.05	0.14	0.55
Gender, Male	38 (50.7%)	4 (30.8%)	15 (48.4%)	19 (61.3%)	0.17	0.34	0.06	0.31
BSA (kg/m ²)	1.8 ± 0.2	1.7 ± 0.2	1.8 ± 0.2	1.8 ± 0.2	0.38	0.59	0.20	0.33
Heart rate (bpm)	66.4 ± 10.6	63.8 ± 6.6	67.2 ± 13.4	66.6 ± 8.8	0.61	0.33	0.43	0.81
LVEDV	129.1 ± 25.5	120.9 ± 26.8	130.9 ± 27.8	130.8 ± 22.7	0.45	0.24	0.25	0.99
LVESV	48.5 ± 12.6	42.8 ± 9.7	49.8 ± 13.3	49.7 ± 12.6	0.20	0.10	0.10	0.98
LVSV	80.6 ± 17.1	78.0 ± 21.0	81.1 ± 16.6	81.1 ± 17.1	0.84	0.58	0.60	0.98
LVEF	62.5 ± 5.7	64.3 ± 5.9	62.2 ± 4.4	62.0 ± 6.7	0.46	0.28	0.23	0.88
LVCO	5.3 ± 1.2	4.9 ± 1.1	5.3 ± 1.1	5.4 ± 1.2	0.44	0.25	0.23	0.93
LVCI	3.0 ± 0.6	2.8 ± 0.5	3.0 ± 0.6	3.0 ± 0.6	0.54	0.27	0.50	0.59
LV mass	76.7 ± 15.1	72.5 ± 14.5	74.3 ± 15.4	80.7 ± 14.7	0.14	0.72	0.10	0.97
LVEDV/BSA	72.4 ± 11.7	69.3 ± 10.6	73.8 ± 12.7	72.4 ± 11.2	0.52	0.25	0.43	0.63
LVESV/BSA	27.1 ± 6.4	24.7 ± 5.1	27.8 ± 6.4	27.5 ± 6.8	0.31	0.14	0.19	0.85
LVSV/BSA	45.3 ± 7.9	44.6 ± 8.6	46.0 ± 7.8	44.8 ± 7.9	0.81	0.60	0.93	0.57
LVCO/BSA	3.0 ± 0.6	2.8 ± 0.5	3.0 ± 0.6	3.0 ± 0.6	0.49	0.24	0.44	0.59
LV mass/BSA	42.9 ± 5.6	41.6 ± 5.6	41.8 ± 5.4	44.4 ± 5.7	0.13	0.91	0.13	0.07
RVEDV	128.8 ± 31.5	118.1 ± 32.8	129.6 ± 34.2	133.5 ± 27.9	0.34	0.31	0.14	0.54
RVESV	54.4 ± 18.3	47.3 ± 15.0	56.7 ± 21.3	55.0 ± 16.1	0.30	0.13	0.20	0.73
RVSV	74.5 ± 18.7	70.8 ± 22.6	72.1 ± 19.2	78.5 ± 16.1	0.30	0.84	0.22	0.18
RVEF	58.1 ± 7.7	59.5 ± 8.6	56.6 ± 8.3	59.1 ± 6.5	0.35	0.26	0.89	0.20
RVCO	4.9 ± 1.2	4.5 ± 1.3	4.8 ± 1.3	5.2 ± 1.0	0.16	0.46	0.08	0.18
RVCI	2.8 ± 0.6	2.6 ± 0.7	2.7 ± 0.7	2.8 ± 0.5	0.40	0.40	0.18	0.51
RVEDV/BSA	71.3 ± 13.8	67.6 ± 14.4	72.4 ± 15.2	71.81 ± 12.23	0.569	0.30	0.36	0.87
RVESV/BSA	30.4 ± 9.1	27.0 ± 7.0	31.8 ± 10.3	30.5 ± 8.4	0.30	0.12	0.25	0.61
RVSV/BSA	41.5 ± 9.0	40.5 ± 10.9	40.8 ± 9.5	42.6 ± 7.9	0.68	0.94	0.50	0.44
RVCO/BSA	2.7 ± 0.6	2.6 ± 0.7	2.7 ± 0.7	2.9 ± 0.5	0.32	0.50	0.15	0.33
Native T1 (ms)	–	1286 ± 60	1253 ± 55	–	0.09	–	–	–
3D-Strain								
LV peak GRS	42.6 ± 19.5	40.5 ± 18.7	46.3 ± 23.0	39.8 ± 15.8	0.39	0.37	0.91	0.19
LV peak GCS	– 17.5 ± 6.5	– 15.1 ± 10.3	– 16.7 ± 6.9	– 19.4 ± 3.0	0.08	0.45	0.04	0.10
LV peak GLS	– 12.7 ± 3.3	– 11.9 ± 3.9	– 12.7 ± 3.6	– 13.1 ± 2.8	0.58	0.47	0.30	0.68
RV peak GRS	31.6 ± 12.6	31.4 ± 14.5	28.8 ± 11.1	34.4 ± 10.4	0.16	0.49	0.42	0.06
RV peak GCS	– 11.9 ± 4.2	– 9.4 ± 3.4	– 12.1 ± 4.0	– 12.9 ± 4.3	0.04	0.05	0.01	0.46
RV peak GLS	– 11.3 ± 4.0	– 7.8 ± 4.0	– 12.9 ± 3.0	– 11.3 ± 3.9	0.00	0.003	0.00	0.08

Boldface characters indicate p (adjusted p) < 0.05

BSA body surface area, CI cardiac index, CO cardiac output, EDV end-diastolic volume, EF ejection fraction, ESV end-systolic volume, GCS global circumferential strain, GLS global longitudinal strain, GRS global radial strain, LGE late gadolinium enhancement, LV left ventricle, RV right ventricle, SV stroke volume

* P-value is for patients with LGE-positive versus patients with LGE-negative versus normal controls

** Adjusted P-value: Statistical difference between patients with and without LGE on CMR imagings

*** P-value: Statistical difference between patients with LGE-positive on CMR imagings and normal controls

**** P-value: Statistical difference between patients with LGE-negative on CMR imagings and normal controls

mL, CRP: 43.0 ± 42.9 mg/L, serum potassium: 3.8 ± 0.3 mmol/L, serum calcium: 1.3 ± 0.2 mmol/L. TnI in LGE group and non-LGE group were 0.02 (0.01–0.04) and 0.01 (0.01–0.02), respectively, with significant difference between the two groups (p < 0.05). (Table 1).

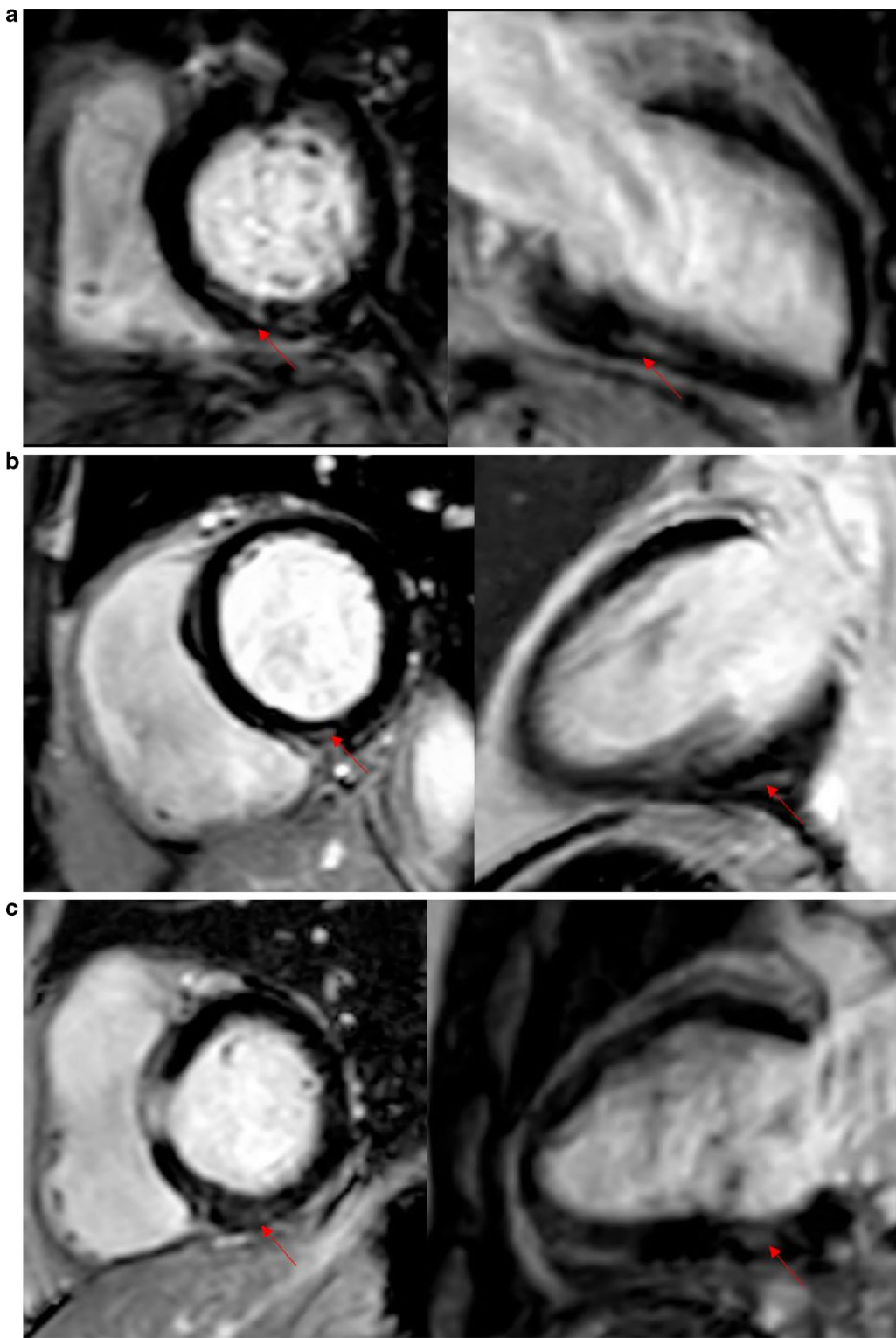


Fig. 1 Illustration of all 13 late gadolinium enhancement (LGE) positive patients' myocardial injury. **a–m** represents case 1–13, respectively. One short axis and orthogonal long-axis phase sensitive inversion recovery (PSIR) images show LGE (arrow) for each patient. *PSIR* phase-sensitive inversion recovery, *LGE* late gadolinium enhancement

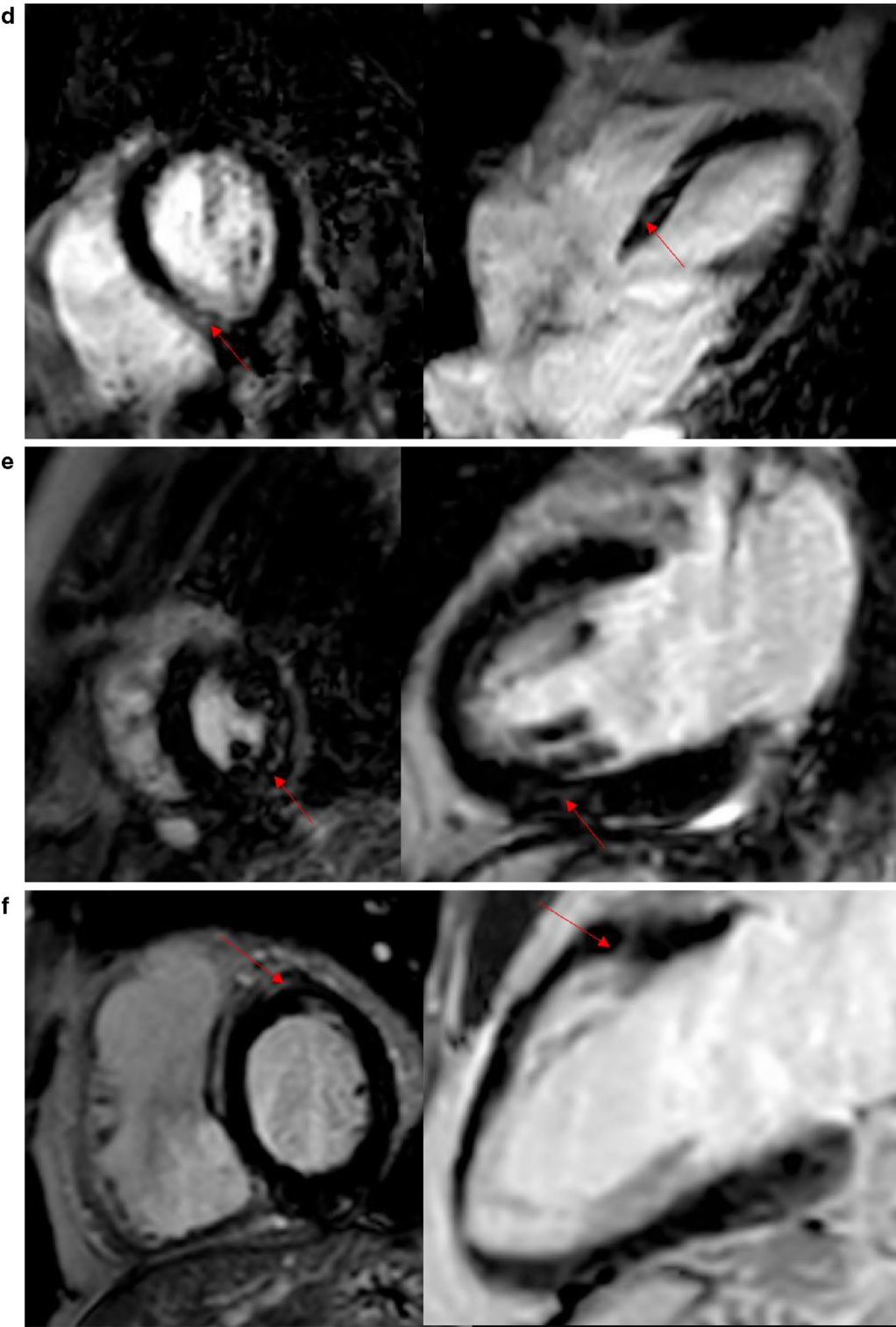


Fig. 1 continued

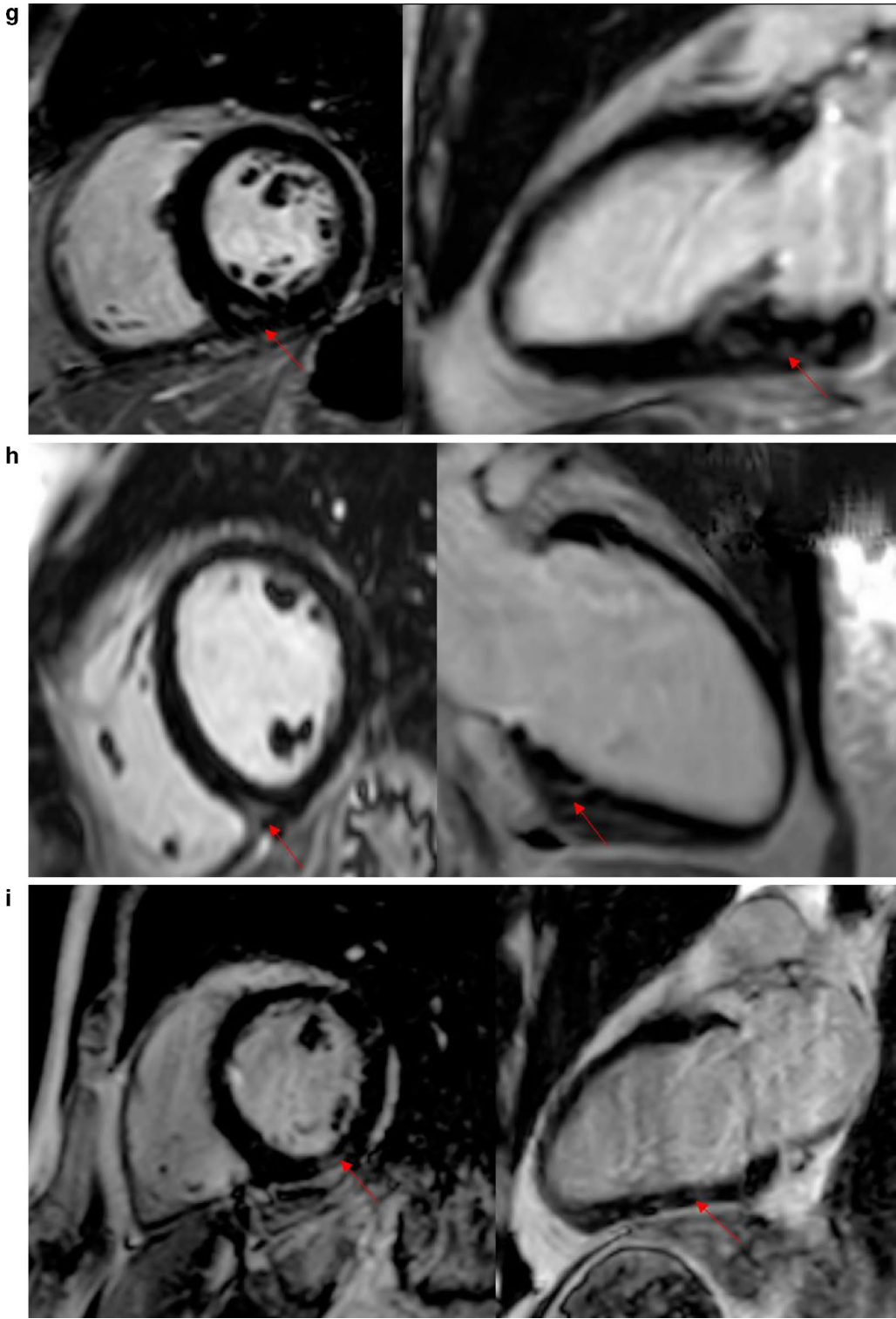


Fig. 1 continued

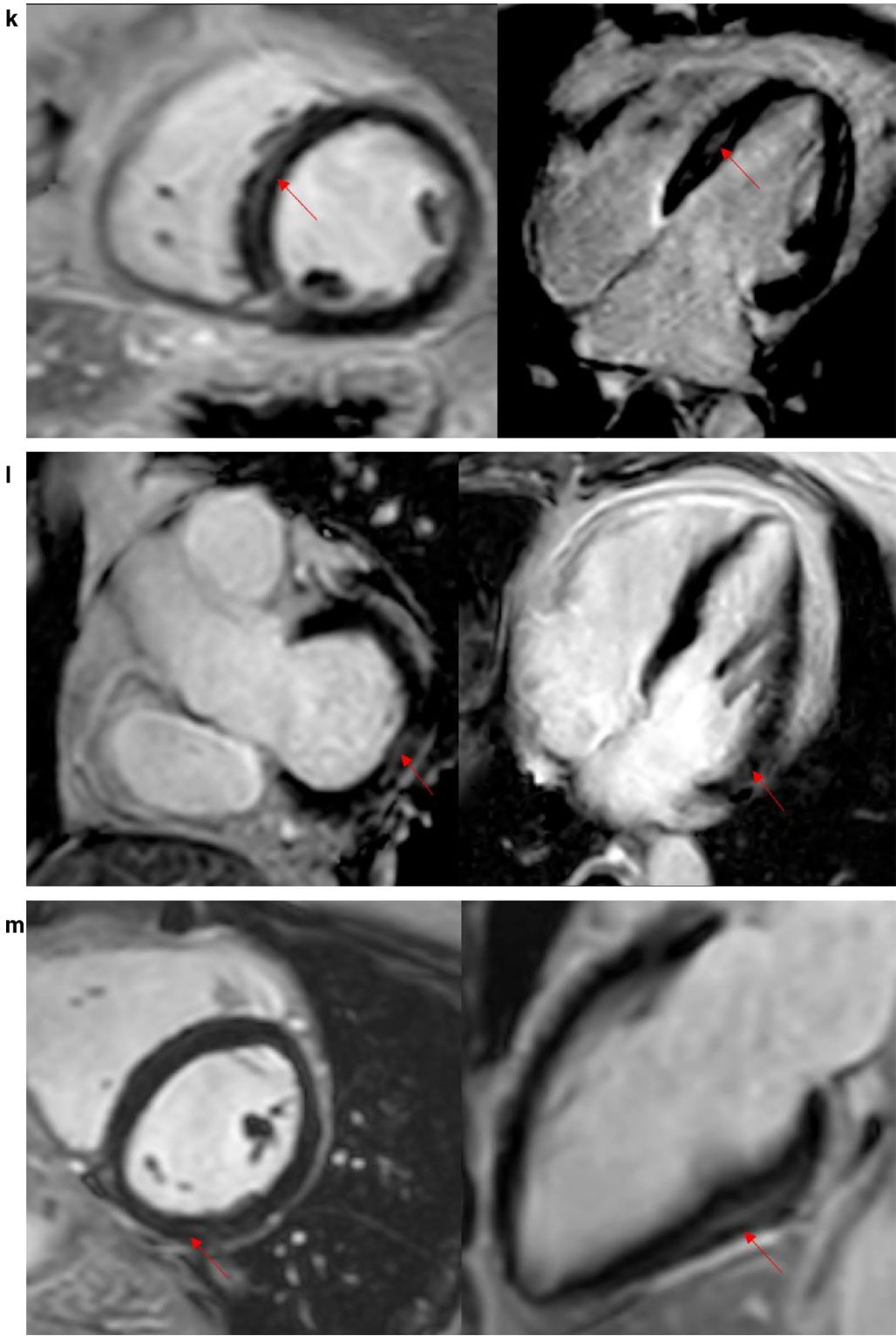


Fig. 1 continued

CMR results

LGE and T1 mapping

No myocardium hemorrhage was observed in any patient; however, LGE was detected in 13 patients (29.5%). All of the LGE-positive patients were from the COVID-19 group, no LGE was observed any of the healthy controls. All LGE lesions were located in the middle myocardium and/or sub-epicardium with a scattered distribution (Fig. 1). Case 1 was the only patient with abnormal ECG findings. Among a total of 208 myocardial segments in 13 patients, most LGE lesions were located at the inferior and inferior-lateral segments at the base and mid-chamber. The Bull's eye illustration (Fig. 2) shows us the number of myocardial LGE distributed in the American Heart Association 16 segments' model for all 13 patients. The inferior wall and inferior-lateral wall of the basal segment was the most frequently involved segment (10/12 patients). The median of LGE/myocardium ratio was 1.7% (1.1–3.0%).

Global native T1 showed no significant difference between COVID-19 patients with and without LGE (1286 ms \pm 60 ms vs 1253 ms \pm 55 ms, $P > 0.05$).

LV/RV morphological, function, and strain analysis

Table 2 shows the values for global LV and RV morphological and functional parameters and the measurement of the 3D global CMR feature-tracking deformation parameters. No significant difference was detected in the LV and RV morphological parameters (EDV, ESV,

and mass) among COVID-19 patients with and without LGE and normal controls. Although no significant difference was detected in the LV and RV traditional function parameters—EF, CO, cardiac index (CI), SV; LV peak GCS was decreased in COVID-19 patients with visual LGE (-15.1 ± 10.3) on CMR images as compared to healthy controls (-19.4 ± 3.0) ($p < 0.05$). Both peak 3D GCS and GLS of RV in COVID-19 patients with LGE (-9.4 ± 3.4 and -7.8 ± 4.0 , respectively) were significantly decreased as compared to COVID-19 patients without LGE (-12.1 ± 4.0 and -12.9 ± 3.0 , respectively) and normal control (-12.9 ± 4.3 and -11.3 ± 3.9 , respectively) (both $p < 0.05$). However, no difference (peak 3D GCS and GLS of RV) was detected between COVID-19 patients without LGE and the normal controls ($p > 0.05$).

Intra-observer ICC of LV peak 3D-GCS, RV peak 3D-GCS and RV peak 3D-GLS were 0.93, 0.92 and 0.77 respectively. Inter-observer ICC of LV peak 3D-GCS, RV peak 3D-GCS and RV peak 3D-GLS were 0.82, 0.70 and 0.76 respectively.

Discussion

The present prospective study among recovered COVID-19 patients found that ~30% had CMR evidence for myocardial injury (manifested as LGE) at 3-month follow up. LGE-positive patients had a decrease in the LV GCS compared to healthy controls and a significant decrease in the RV GCS and GLS as compared to non-LGE COVID-19 patients.

Myocardial involvement has been proved to be one of the primary manifestations of COVID-19 infection by laboratory, autopsy, and CMR [14–16] as compared to other members of the coronavirus family [17]. A recent study demonstrated that in the recovered COVID-19 patients with cardiac symptoms, 54% had myocardium edema, and 31% had LGE [11]. The persistence of visual LGE at 3-month follow-up reflecting necrosis or scar (fibrosis) might be caused by COVID-19 and needs to be elucidated further [18]. Yet, visual LGE indicated that up to 30% COVID-19 patients have irreversible myocardial injury [19, 20], which is consistent with the findings of the previous study and can confirm one of the main mechanisms of COVID-19 induced direct myocardial injury—myocarditis [21–23]. In addition, the presence of LGE has been proven to be an independent predictor of all-cause mortality and cardiac mortality in myocarditis [24, 25]. Since the LGE/myocardium ratio was small, the cardiac status of COVID-19 patients with LGE needs to be closely monitored.

We found all of the LGE lesions to be located in the middle myocardium and/or sub-epicardium, wherein the fibers are oriented transversely, and the torque enhances

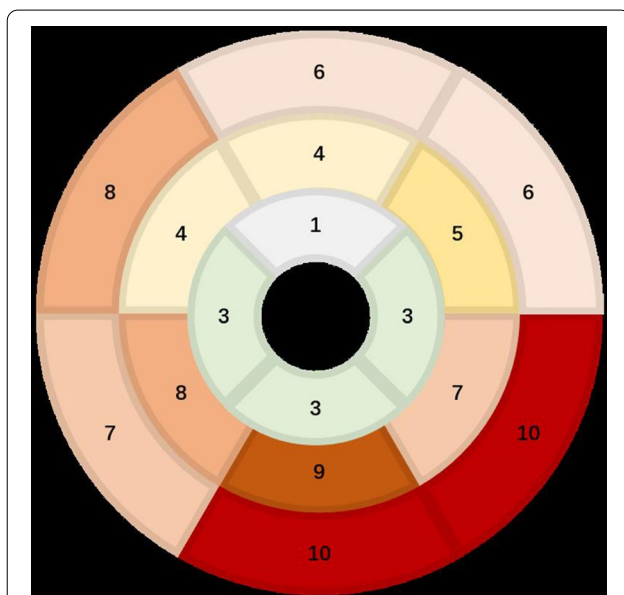


Fig. 2 Dominant distribution of myocardial LGE segments in recovered COVID-19 patients. Number of myocardial LGE distributed in American Heart Association 16 segment model in all the 13 patients

shortening in the circumferential direction [26, 27]. This may be the reason for LV 3D GCS to be oriented along the perimeter in short axis view [26] and decreased in the COVID-19 patients with LGE. This finding prompts us to focus on the LV circumferential contraction dysfunction in these patients in addition to impaired RV function.

Impaired RV function in COVID-19 survivors has been demonstrated by echocardiography and CMR [11, 28, 29]. RV strain has been recommended to assess the RV function in clinical scenarios with suspected RV dysfunction [30]. Although our results showed that the RV traditional morphological and function parameters are in a normal range, the RV strain in COVID-19 patients with LGE was significantly decreased as compared to those without LGE and healthy controls. This phenomenon indicated that COVID-19 patients with LGE still had RV dysfunction, which could be detected by CMR strain analysis. COVID-19 results in acute respiratory distress syndrome (ARDS) [31] and is frequently associated with RV dysfunction, increased pulmonary resistance [32], increased values of systolic pulmonary arterial pressure, increased RV afterload [33, 34], severe hypoxia, oxidative stress, and increased myocardial oxygen demand induced by ARDS [35].

According to a recent systematic echocardiographic study, the most frequent abnormality induced by COVID-19 was RV dilation with or without dysfunction [32]. However, our results only showed RV dysfunction in patients with LGE. No RV morphological (EDV and ESV) difference was detected at the 3-month follow up, which might be attributed to improved pneumonia; subsequently, the RV rapidly returns to normal size while the RV strain is still decreased. Global native T1 value in both LGE-positive and LGE-negative COVID-19 patients were elevated compared with [1122 (1100, 1143) ms and 1122 ± 57 ms] healthy subjects, performed at Philips 3 T CMR with MOLLI sequence, previously reported by Gottbrecht et al. [36] and Clotilde Roy et al [37].

Limitations

The current study has limitations. First, the lack of baseline pre-COVID-19 CMR examination limits the evaluation of the progress of heart involvement. Second, the sample size was relatively small. Third, the majority of the recruited patients had moderate and severe COVID-19, and hence, our study does not reflect the full spectrum of critical COVID-19 patients. Fourth, we had data of only a 3-month CMR examination, and thus, a long-time follow-up is essential to determine the progression or regression of cardiac involvement. Fifth, we did not have native T1 of the healthy control group, which would be useful information to compare with the COVID-19 patients. However, we provide reference normal T1 value base on the previous studies. Sixth, we did not have

information regarding hemodynamic instability or evidence of cardiac involvement during initial diagnosis or hospitalization on all patients, which would be helpful to correlate those kinds of patients with the CMR findings.

Conclusions

Myocardium injury is present in nearly a third of COVID-19 patients at 3 months with evidence of impaired LV GCS and RV GCS and GLS. CMR may be useful to monitor the COVID-19-induced myocarditis progress and remains to be examined.

Abbreviations

ACEI: Angiotensin-converting enzyme inhibitor; ARB: Angiotensin receptor blocker; ARDS: Acute respiratory distress syndrome; BSA: Body surface area; bSSFP: Balanced steady state-free precession; CI: Cardiac index; CMR: Cardiovascular magnetic resonance; CO: Cardiac output; COVID-19: Coronavirus disease 2019; CPK: Creatine phosphokinase; CRP: C-reactive protein; ECG: Electrocardiogram; EDV: End-diastolic volume; EF: Ejection fraction; ESV: End-systolic volume; FA: Flip angle; FOV: Field of view; GCS: Global circumferential strain; GLS: Global longitudinal strain; GRS: Global radial strain; IQR: Interquartile range; LGE: Late gadolinium enhancement; LV: Left ventricle/left ventricular; MOLLI: Modified look-locker inversion recovery; MYO: Myohemoglobin; PSIR: Phase-sensitive inversion-recovery; RV: Right ventricle/right ventricular; SI: Signal intensity; SV: Stroke volume; T2w: T2 weighted; TE: Echo time; Tnl: Troponin I; TR: Repetition time; TSE: Turbo spin echo.

Acknowledgements

Not applicable.

Authors' contributions

HW and RLL had full access to all of the data in the study and takes responsibility for the integrity of the data and the accuracy of the data analysis. Study concept and design: LX, HJL. Acquisition of data: HW, RLL, HJ, ZXY, XYT. Analysis and interpretation of data: HW, ZZ, LX. Draft of the manuscript: HW. Critical revision of the manuscript for important intellectual content: LX, HL. Statistical analysis: HW, LX. Study supervision: LX, HJL. All authors read and approved the final manuscript.

Funding

This study was supported by a grants from National Natural Science Foundation of China (U1908211), the National Key Research and Development Program of China (2016YFC1300300), and Capital Medical Development Research Foundation of China (PXM2020_026272_000013) for Dr. L. Xu. And grants from Beijing Municipal Health Commission, Technology Achievements and Appropriate Technology Promotion Project (2020-TG-002) and You'an Medical Development Project of COVID-19 Emergency Prevention and Control Public (BJYAY-2020YC-03) for Dr. HJ. Li.

Availability of data and materials

The datasets used and/or analyzed during the current study are available from the corresponding author on reasonable request.

Ethics approval and consent to participate

The study was approved by the local ethic committees, and all patients gave informed consent for their medical data to be used in this study.

Consent for publication

The manuscript is approved by all authors for publication.

Competing interests

The authors declare that they have no competing interests.

Received: 30 July 2020 Accepted: 7 January 2021

Published online: 25 February 2021

References

- WHO coronavirus disease (COVID-19) dashboard. Geneva: World Health Organization, 2020. <https://covid19.who.int/>. In. 2020/7/4 edn.
- Bavishi C, Bonow RO, Trivedi V, Abbott JD, Messerli FH, Bhatt DL. Acute myocardial injury in patients hospitalized with COVID-19 infection: a review. *Prog Cardiovasc Dis*. 2020. <https://doi.org/10.1016/j.pcad.2020.05.013>.
- Shi S, Qin M, Shen B, Cai Y, Liu T, Yang F, et al. Association of cardiac injury with mortality in hospitalized patients with COVID-19 in Wuhan, China. *JAMA Cardiol*. 2020. <https://doi.org/10.1001/jamacardio.2020.0950>.
- Ruan Q, Yang K, Wang W, Jiang L, Song J. Correction to: clinical predictors of mortality due to COVID-19 based on an analysis of data of 150 patients from Wuhan, China. *Intensive Care Med*. 2020;46:1294–7. <https://doi.org/10.1007/s00134-020-06028-z>.
- Guo T, Fan Y, Chen M, Wu X, Zhang L, He T, et al. Cardiovascular implications of fatal outcomes of patients with coronavirus disease 2019 COVID-19. *JAMA Cardiol*. 2019. <https://doi.org/10.1001/jamacardio.2020.1017>.
- Akhmerov A, Marban E. COVID-19 and the Heart. *Circ Res*. 2020;126:1443–55. <https://doi.org/10.1161/CIRCRESAHA.120.317055>.
- Madjid M, Safavi-Naeini P, Solomon SD, Vardeny O. Potential effects of coronaviruses on the cardiovascular system: a review. *JAMA Cardiol*. 2020. <https://doi.org/10.1001/jamacardio.2020.1286>.
- Clerkin KJ, Fried JA, Raikhelkar J, Sayer G, Griffin JM, Masoumi A, et al. COVID-19 and cardiovascular disease. *Circulation*. 2020;141:1648–55. <https://doi.org/10.1161/CIRCULATIONAHA.120.046941>.
- Cheng R, Leedy D. COVID-19 and acute myocardial injury: the heart of the matter or an innocent bystander? *Heart*. 2020. <https://doi.org/10.1136/heartjnl-2020-317025>.
- Schulz-Menger J, Bluemke DA, Bremerich J, Flamm SD, Fogel MA, Friedrich MG, et al. Standardized image interpretation and post-processing in cardiovascular magnetic resonance—2020 update: Society for Cardiovascular Magnetic Resonance (SCMR): Board of Trustees Task Force on Standardized Post-Processing. *J Cardiovasc Magn Reson*. 2020;22:19. <https://doi.org/10.1186/s12968-020-00610-6>.
- Huang L, Tang D, Zhu T, Han R, Zhan C, Liu W, Zeng H, Tao Q, Xia L. Cardiac involvement in recovered COVID-19 patients identified by magnetic resonance imaging. *JACC Cardiovasc Imaging*. 2020. <https://doi.org/10.1016/j.jcmg.2020.05.004>.
- Grani C, Eichhorn C, Biere L, Kaneko K, Murthy VL, Agarwal V, et al. Comparison of myocardial fibrosis quantification methods by cardiovascular magnetic resonance imaging for risk stratification of patients with suspected myocarditis. *J Cardiovasc Magn Reson*. 2019;21:14. <https://doi.org/10.1186/s12968-019-0520-0>.
- China NHCotPsRo. Diagnosis and Treatment Protocol of Novel Coronavirus (trial version 6th). National Health Commission of the People's Republic of China Website <http://www.nhc.gov.cn/xcs/zhengcwj/202003/4856d5b0458141fa9f376853224d41d7s.html>. 2020.
- Buja LM, Wolf DA, Zhao B, Akkanti B, McDonald M, Lelenwa L, et al. The emerging spectrum of cardiopulmonary pathology of the coronavirus disease 2019 (COVID-19): report of 3 autopsies from Houston, Texas, and review of autopsy findings from other United States cities. *Cardiovasc Pathol*. 2020;48:107233. <https://doi.org/10.1016/j.carpath.2020.107233>.
- Gravinay P, Issa N, Girard D, Camou F, Cochet H. CMR and serology to diagnose COVID-19 infection with primary cardiac involvement. *Eur Heart J Cardiovasc Imaging*. 2020. <https://doi.org/10.1093/ehjci/jeaa169>.
- Han H, Xie L, Liu R, Yang J, Liu F, Wu K, et al. Analysis of heart injury laboratory parameters in 273 COVID-19 patients in one hospital in Wuhan, China. *J Med Virol*. 2020;92:819–23. <https://doi.org/10.1002/jmv.25809>.
- Ansari Ramandi MM, Baay M, Naderi N. Does the novel coronavirus 2019 like heart more than the other family members of coronaviruses? *J Cardiovasc Thorac Res*. 2020;12:156–7. <https://doi.org/10.34172/jcvtr.2020.27>.
- Berg J, Kottwitz J, Baltensperger N, Kissel CK, Lovrinovic M, Mehra T, et al. Cardiac magnetic resonance imaging in myocarditis reveals persistent disease activity despite normalization of cardiac enzymes and inflammatory parameters at 3-month follow-up. *Circ Heart Fail*. 2017. <https://doi.org/10.1161/CIRCHEARTFAILURE.117.004262>.
- Luetkens JA, Homsí R, Dabir D, Kuetting DL, Marx C, Doerner J, et al. Comprehensive cardiac magnetic resonance for short-term follow-up in acute myocarditis. *J Am Heart Assoc*. 2016. <https://doi.org/10.1161/JAHA.116.003603>.
- Zagrosek A, Abdel-Aty H, Boye P, Wassmuth R, Messroghli D, Utz W, et al. Cardiac magnetic resonance monitors reversible and irreversible myocardial injury in myocarditis. *JACC Cardiovasc Imaging*. 2009;2:131–8. <https://doi.org/10.1016/j.jcmg.2008.09.014>.
- Rali AS, Ranka S, Shah Z, Sauer AJ. Mechanisms of myocardial injury in coronavirus disease 2019. *Card Fail Rev*. 2020;6:e15. <https://doi.org/10.15420/cfr.2020.10>.
- Dhakal BP, Sweitzer NK, Indik JH, Acharya D, William P. SARS-CoV-2 infection and cardiovascular disease: COVID-19 heart. *Heart Lung Circ*. 2020. <https://doi.org/10.1016/j.hlc.2020.05.101>.
- Babapoor-Farrokh S, Gill D, Walker J, Rasekhi RT, Bozorgnia B, Amanullah A. Myocardial injury and COVID-19: possible mechanisms. *Life Sci*. 2020;253:117723. <https://doi.org/10.1016/j.lfs.2020.117723>.
- Grun S, Schumm J, Greulich S, Wagner A, Schneider S, Bruder O, et al. Long-term follow-up of biopsy-proven viral myocarditis: predictors of mortality and incomplete recovery. *J Am Coll Cardiol*. 2012;59:1604–15. <https://doi.org/10.1016/j.jacc.2012.01.007>.
- Barone-Rochette G, Augier C, Rodiere M, Quesada JL, Foote A, Bouvaist H, et al. Potentially simple score of late gadolinium enhancement cardiac MR in acute myocarditis outcome. *J Magn Reson Imaging*. 2014;40:1347–54. <https://doi.org/10.1002/jmri.24504>.
- Jeung MY, Germain P, Croisille P, El Ghannudi S, Roy C, Gangi A. Myocardial tagging with MR imaging: overview of normal and pathologic findings. *Radiographics*. 2012;32:1381–98. <https://doi.org/10.1148/rq.325115098>.
- Sengupta PP, Tajik AJ, Chandrasekaran K, Khandheria BK. Twist mechanics of the left ventricle: principles and application. *JACC Cardiovasc Imaging*. 2008;1:366–76. <https://doi.org/10.1016/j.jcmg.2008.02.006>.
- Mahmoud-Elsayed HM, Moody WE, Bradlow WM, Khan-Kheil AM, Senior J, Hudsmith LE, et al. Echocardiographic findings in patients with COVID-19 pneumonia. *Can J Cardiol*. 2020. <https://doi.org/10.1016/j.cjca.2020.05.030>.
- Sud K, Vogel B, Bohra C, Garg V, Talebi S, Lerakis S, et al. Echocardiographic findings in patients with COVID-19 with significant myocardial injury. *J Am Soc Echocardiogr*. 2020. <https://doi.org/10.1016/j.echo.2020.05.030>.
- Claus P, Omar AMS, Pedrizzetti G, Sengupta PP, Nagel E. Tissue tracking technology for assessing cardiac mechanics: principles, normal values, and clinical applications. *JACC Cardiovasc Imaging*. 2015;8:1444–60. <https://doi.org/10.1016/j.jcmg.2015.11.001>.
- Chen N, Zhou M, Dong X, Qu J, Gong F, Han Y, et al. Epidemiological and clinical characteristics of 99 cases of 2019 novel coronavirus pneumonia in Wuhan, China: a descriptive study. *Lancet*. 2020;395:507–13. [https://doi.org/10.1016/S0140-6736\(20\)30211-7](https://doi.org/10.1016/S0140-6736(20)30211-7).
- Szekely Y, Lichter Y, Taieb P, Banai A, Hochstadt A, Merdler I, et al. The spectrum of cardiac manifestations in coronavirus disease 2019 (COVID-19)—a systematic echocardiographic study. *Circulation*. 2019. <https://doi.org/10.1161/CIRCULATIONAHA.120.047971>.
- Bouferrache K, Vieillard-Baron A. Acute respiratory distress syndrome, mechanical ventilation, and right ventricular function. *Curr Opin Crit Care*. 2011;17:30–5. <https://doi.org/10.1097/MCC.0b013e328342722b>.
- Bonizzoli M, Cipani S, Lazzeri C, Chiostrì M, Ballo P, Sarti A, et al. Speckle tracking echocardiography and right ventricle dysfunction in acute respiratory distress syndrome a pilot study. *Echocardiography*. 2018;35:1982–7. <https://doi.org/10.1111/echo.14153>.
- Tahir F, Bin Arif T, Ahmed J, Malik F, Khalid M. Cardiac manifestations of coronavirus disease 2019 (COVID-19): a comprehensive review. *Cureus*. 2020;12:e8021. <https://doi.org/10.7759/cureus.8021>.
- Gottbrecht M, Kramer CM, Salerno M. Native T1 and extracellular volume measurements by cardiac MRI in healthy adults: a meta-analysis. *Radiology*. 2019;290:317–26. <https://doi.org/10.1148/radiol.2018180226>.
- Roy C, Slimani A, de Meester C, Amzulescu M, Pasquet A, Vancraeynest D, et al. Age and sex corrected normal reference values of T1, T2 T2* and ECV in healthy subjects at 3T CMR. *J Cardiovasc Magn Reson*. 2017;19:72. <https://doi.org/10.1186/s12968-017-0371-5>.

Publisher's Note

Springer Nature remains neutral with regard to jurisdictional claims in published maps and institutional affiliations.